

ORIGINAL ARTICLE

PPAR agonist-mediated protection against HIV Tat-induced cerebrovascular toxicity is enhanced in MMP-9-deficient mice

Wen Huang¹, Lei Chen², Bei Zhang³, Minseon Park⁴ and Michal Toborek⁴

The strategies to protect against the disrupted blood–brain barrier (BBB) in HIV-1 infection are not well developed. Therefore, we investigated the potential of peroxisome proliferator-activated receptor (PPAR) agonists to prevent enhanced BBB permeability induced by HIV-1-specific protein Tat. Exposure to Tat via the internal carotid artery (ICA) disrupted permeability across the BBB; however, this effect was attenuated in mice treated with fenofibrate (PPAR α agonist) or rosiglitazone (PPAR γ agonist). In contrast, exposure to GW9662 (PPAR γ antagonist) exacerbated Tat-induced disruption of the BBB integrity. Increased BBB permeability was associated with decreased tight junction (TJ) protein expression and activation of ERK1/2 and Akt in brain microvessels; these effects were attenuated by cotreatment with fenofibrate but not with rosiglitazone. Importantly, both PPAR agonists also protected against Tat-induced astrogliosis and neuronal loss. Because disruption of TJ integrity has been linked to matrix metalloproteinase (MMP) activity, we also evaluated Tat-induced effects in MMP-9-deficient mice. Tat-induced cerebrovascular toxicity, astrogliosis, and neuronal loss were less pronounced in MMP-9-deficient mice as compared with wild-type controls and were further attenuated by PPAR agonists. These results indicate that enhancing PPAR activity combined with targeting MMPs may provide effective therapeutic strategies in brain infection by HIV-1.

Journal of Cerebral Blood Flow & Metabolism (2014) **34**, 646–653; doi:10.1038/jcbfm.2013.240; published online 15 January 2014

Keywords: blood–brain barrier; human immunodeficiency virus-1; matrix metalloproteinase; peroxisome proliferator-activated receptor; Tat protein; neurotoxicity

INTRODUCTION

Highly active antiretroviral therapy significantly prolongs the lives of HIV-infected patients. While the overall severity of HIV-associated neurocognitive disorders decreased reflecting a better virologic control, neurocognitive impairment remained prevalent or even increased.¹ This phenomenon may be related to the fact that HIV-infected patients live longer and aging becomes an important comorbidity factor contributing to neurocognitive deficits in HIV infection.² In addition, the brain is considered to be an important HIV reservoir, which is relatively poorly accessed by antiretroviral drugs;¹ thus, HIV may replicate in the brain even though HIV replication is suppressed in the periphery. Another hypothesis explaining the persistent high prevalence of neurocognitive dysfunction is related to the toxicity of antiretroviral drugs. For example, protease inhibitors induce alterations in plasma lipids and insulin levels that place patients at the risk for coronary heart disease and cerebral vascular disease.^{3,4} Highly active antiretroviral therapy, including nucleoside reverse transcriptase inhibitors, can increase the intracellular reactive oxygen species production,⁵ supporting the rationale for supplementary antioxidative therapy.

Peroxisome proliferator-activated receptors (PPARs) are ligand-activated transcription factors that are considered to be critical rescue molecules, which can downregulate activation of

redox-responsive transcription factors and exert antiinflammatory effects. We and others observed that PPARs can protect against HIV-1-induced neuroinflammation and dysfunction of brain endothelial cells partly by inhibition of proinflammatory responses.^{6–8} Study indicates that PPAR γ agonist rosiglitazone may also partly correct lipoatrophy in patients with HIV infection.⁷ Rosiglitazone can reduce HIV-1 replication in lymphocytes and brain macrophages, offering a new therapeutic intervention to HIV-1 infection in central nervous system (CNS).⁹

HIV-1 infection is associated with increased expression and activity of matrix metalloproteinases (MMPs) in the CNS, with elevated levels of MMP-9 being reported in cerebrospinal fluid of HIV-1-infected patients.^{10,11} Imbalance between MMPs and endogenous TIMPs (tissue inhibitors of MMPs) may contribute to HIV-associated pathology by inducing remodeling of the extracellular matrix.¹² Activation of ERK1/2- and JNK-NF- κ B cascades by reactive oxygen species appears to be essential for MMP-9 upregulation.¹³ We reported that overexpression of PPARs attenuated HIV-1-mediated dysregulation of tight junctions (TJs) by inhibiting MMP activity and caveolae-associated ERK and Akt signaling *in vitro*.^{14,15} However, MMP activity was also linked to neuronal loss.¹⁶ In fact, it was showed that Tat-induced neurotoxicity can be prevented by an MMP inhibitor, prinomastat, and upregulation of TIMP-1 by glia in acute HIV-1 infection may exhibit neuroprotection.¹⁷

¹Department of Neurology, The First Affiliated Hospital of Guangxi Medical University, Nanning, China; ²Department of Neuroscience, Mount Sinai School of Medicine, New York, New York, USA; ³Spinal Cord and Brain Injury Research Center, University of Kentucky, Lexington, Kentucky, USA and ⁴Department of Biochemistry and Molecular Biology, University of Miami School of Medicine, Miami, Florida, USA. Correspondence: Dr M Toborek, Department of Biochemistry and Molecular Biology, University of Miami School of Medicine, Gautier Building, Room 528, 1011 NW 15th Street, Miami, FL 33136, USA. E-mail: mtoborek@med.miami.edu

This work was supported by the National Institutes of Health grants MH063022, MH098891, MH072567, DA027569, and CA133257, the American Heart Association grant AHA09POST2060217, the National Nature Science Foundation of China (81160152, 81371333), and Guangxi Nature Science Foundation (2013GXNSFCA019013). Tat was produced and provided by support from the National Center for Research Resources (Grant # P20 RR15592).

Received 7 August 2013; revised 15 November 2013; accepted 25 November 2013; published online 15 January 2014

Because targeting both PPAR and MMP activities may alleviate HIV-1-induced neuropathology, we focused the present study on the interactions of these factors in a model of HIV cerebral toxicity induced by HIV-specific protein Tat. Our data indicate that Tat-induced disruption of the blood–brain barrier (BBB), alterations in TJ protein expression as well as neuronal loss and astrogliosis can be attenuated by PPAR agonists and MMP-9 deficiency. Importantly, combining these factors offered superior therapeutic advantages.

MATERIALS AND METHODS

Animals and Treatment

Wild-type (WT) (FVB/NJ) and MMP-9-deficient mice (3 months old, males), generated on the FVB/NJ genetic background, were purchased from the Jackson Laboratory (Bar Harbor, ME, USA). All experiments were performed in strict adherence to the National Institutes of Health Guide for the Care and Use of Laboratory Animals. All procedures and protocols were approved by the University of Kentucky Institutional Animal Care and Use Committee. Mice ($n=3$ per group) were administered intraperitoneally once daily for 7 days with fenofibrate (PPAR α agonist, 100 mg/kg), rosiglitazone (PPAR γ agonist, 10 mg/kg), MK886 (PPAR α antagonist, 3 mg/kg), or GW9662 (PPAR γ antagonist, 1 mg/kg). Fenofibrate and rosiglitazone were obtained from Sigma (St. Louis, MO, USA) and MK886 and GW9662 from Alexis Biochemicals (San Diego, CA, USA). All PPAR agonists and antagonists were dissolved in dimethyl sulfoxide/saline (1:10).

At the end of the treatment period with PPAR agonists, HIV-1-specific Tat protein (or vehicle in control mice) was delivered via the internal carotid artery (ICA) and allowed to circulate for 24 hours as established by our group.¹⁸ Under these experimental conditions, administration of heat inactivated Tat has no biologic activity.¹⁹ The route of Tat delivery via the ICA is a model of Tat being released from HIV-infected blood-borne cells and affecting the BBB from the luminal site of the brain endothelium. In specific experiments, Tat was administered every other day for a total of three injections. Recent study estimated Tat levels up to 40 ng/mL in the cerebrospinal fluid of HIV-infected individuals on antiretroviral therapy.²⁰ We exposed mice to Tat based on dose-dependent experiments in which 20 μ g/injection was effective in disruption of the BBB.²¹ However, only a small fraction of administered Tat is likely to be bioavailable, as Tat can be sequestered by endogenous antibodies and extracellular matrices. In addition, Tat polymerizes easily due to the presence of seven cysteine residues, but only the monomeric form is biologically active. Furthermore, the Tat molecule has five arginine residues that make the protein stick easily to plastic and glass, further decreasing its bioavailability.

Blood–Brain Barrier Permeability Assay

Blood–brain barrier integrity was assessed as described earlier.²¹ Briefly, mice were injected intraperitoneally with 200 μ L sodium fluorescein (6 mg/mL, in sterile phosphate-buffered saline, PBS), which was allowed to circulate for 20 minutes. Mice were anesthetized with isoflurane in oxygen, blood was collected through heart puncture, and centrifuged for segregating plasma. Mice were perfused through the left ventricle with 30 mL PBS. Brains were homogenized in PBS (1:10, w/v) and centrifuged at 14,000 g for 2 minutes. Then, 15% trichloroacetic acid (500 μ L) was added to the supernatants (500 μ L) and the mixtures were at 1,000 g for 10 minutes. The supernatants (500 μ L) were neutralized with 125 μ L NaOH (5 mol/L). Fluorescence was measured in 200 μ L aliquots of neutralized brain homogenates using 485 nm and 530 nm for excitation and emission, respectively. Plasma was diluted with PBS (1:100) and measured for fluorescence intensity using the same setting. The BBB permeability was calculated as the ratio of sodium fluorescein in the brain to plasma.

Expression of Akt, ERK1/2, and Tight Junction Proteins in Brain Microvessels

Brain microvessels were isolated 24 hours after Tat injection using a previously described procedure.²² Briefly, mice were anesthetized with isoflurane in oxygen, and perfused with 15 mL saline. After decapitation, the brains were removed and immediately immersed in ice-cold isolation buffer with Complete Protease Inhibitor (Roche, Indianapolis, IN, USA). Choroid plexus, meninges, cerebellum, and brain stem were removed; the brains were homogenized in isolation buffer with Complete Protease Inhibitor, followed by dextran gradient centrifugation. The obtained pellets

containing microvessels were either smeared on slides for immunofluorescent staining or resuspended in 0.5 mL of 6 mol/L urea lysis buffer (6 mol/L urea, 0.1% Triton X-100, 10 mmol/L Tris, pH 8.0, 5 mmol/L MgCl₂, 5 mmol/L EDTA, 150 mmol/L NaCl) with Complete Protease Inhibitor for immunoblotting analyses. Protein samples were either immediately used or stored at -80°C .²²

For immunoblotting, protein samples were separated on 4% to 15% Tris-HCl Ready SDS-polyacrylamide gel (Bio-Rad Laboratories, Hercules, CA, USA), blotted onto polyvinylidene difluoride membranes (Bio-Rad Laboratories), and incubated with the respective antibodies.^{18,22} Anti-zonula occludens-1 (ZO-1) and claudin-5 antibodies were purchased from Zymed (San Francisco, CA, USA). Anti-total-ERK1/2 (T-ERK1/2, p44/42 MAPK), phospho-ERK1/2 (pERK1/2), and phospho-Akt (Ser473; D9E) antibodies were from Cell Signaling (Danvers, MA, USA). Anti-actin antibody was from Sigma. Anti-Akt1/2/3 (H-136) and all secondary antibodies were from Santa Cruz Biotechnology (Santa Cruz, CA, USA). Immunoblots were analyzed using an ECL Western blot detection kit (GE Healthcare Life Sciences, Piscataway, NJ, USA) and proteins of interest were semiquantitated with the ImageJ software (NIH, Baltimore, MD, USA).

For immunofluorescent staining, brain microvessels smeared on slides were fixed for 10 minutes at 95°C , followed by incubation with 3% formaldehyde in PBS for 10 minutes at 25°C . Slides were washed five times with PBS, permeabilized with 0.1% Triton X-100 for 30 minutes, rewashed five times in PBS, and blocked in 1% bovine serum albumin (BSA) in PBS for 30 minutes at 25°C . Samples were then incubated with an individual primary antibody (1:500 dilutions in 1% BSA in PBS) overnight at 4°C . Slides were washed with PBS and incubated with Alexafluor 568-conjugated anti-mouse IgG or Alexafluor 488-conjugated anti-rabbit IgG (Invitrogen, Carlsbad, CA, USA) (1:1,000 dilution in 1% BSA in PBS) for 1 hour at 37°C . After final washing with PBS, slides were mounted with ProLong Gold Antifade reagent containing 4',6-diamidino-2-phenylindole (Invitrogen) to visualize the nuclei. The immunofluorescent images were evaluated and captured using confocal microscopy.

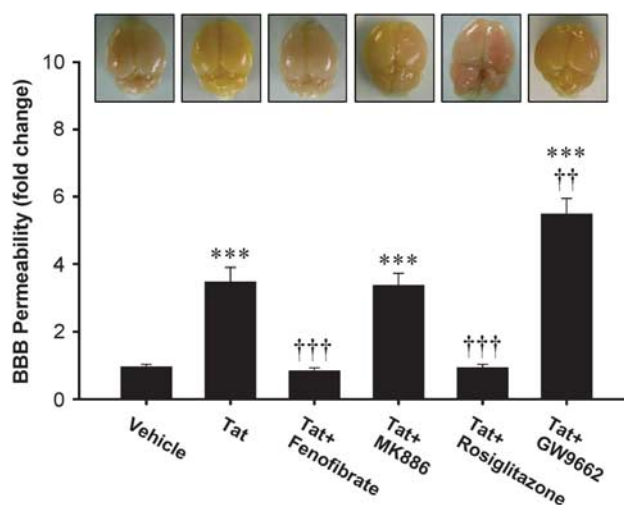


Figure 1. Peroxisome proliferator-activated receptor (PPAR) agonists protect against HIV-1 Tat-induced disruption of blood–brain barrier (BBB) integrity. Wild-type (FVB/NJ) mice were administered intraperitoneally with vehicle, fenofibrate (PPAR α agonist, 100 mg/kg), rosiglitazone (PPAR γ agonist, 10 mg/kg), MK886 (PPAR α antagonist, 3 mg/kg), or GW9662 (PPAR γ antagonist, 1 mg/kg) once a day for 1 week, followed by injection with Tat (20 μ g/mouse) via the internal carotid artery (ICA). The BBB permeability was assessed 24 hours after Tat administration using sodium fluorescein as the marker, which macroscopically stains the brains with highly disrupted BBB in yellow (upper panel). Quantification of the effects of Tat and PPAR modulators on the BBB permeability are shown as a bar graph. Results are the mean \pm SEM. ***Significantly different as compared with vehicle-treated controls at $***P<0.001$. †††Results in the groups exposed to Tat plus PPAR agonist or antagonist are significantly different as compared with the group exposed only to Tat at $P<0.01$ or $†††P<0.001$.

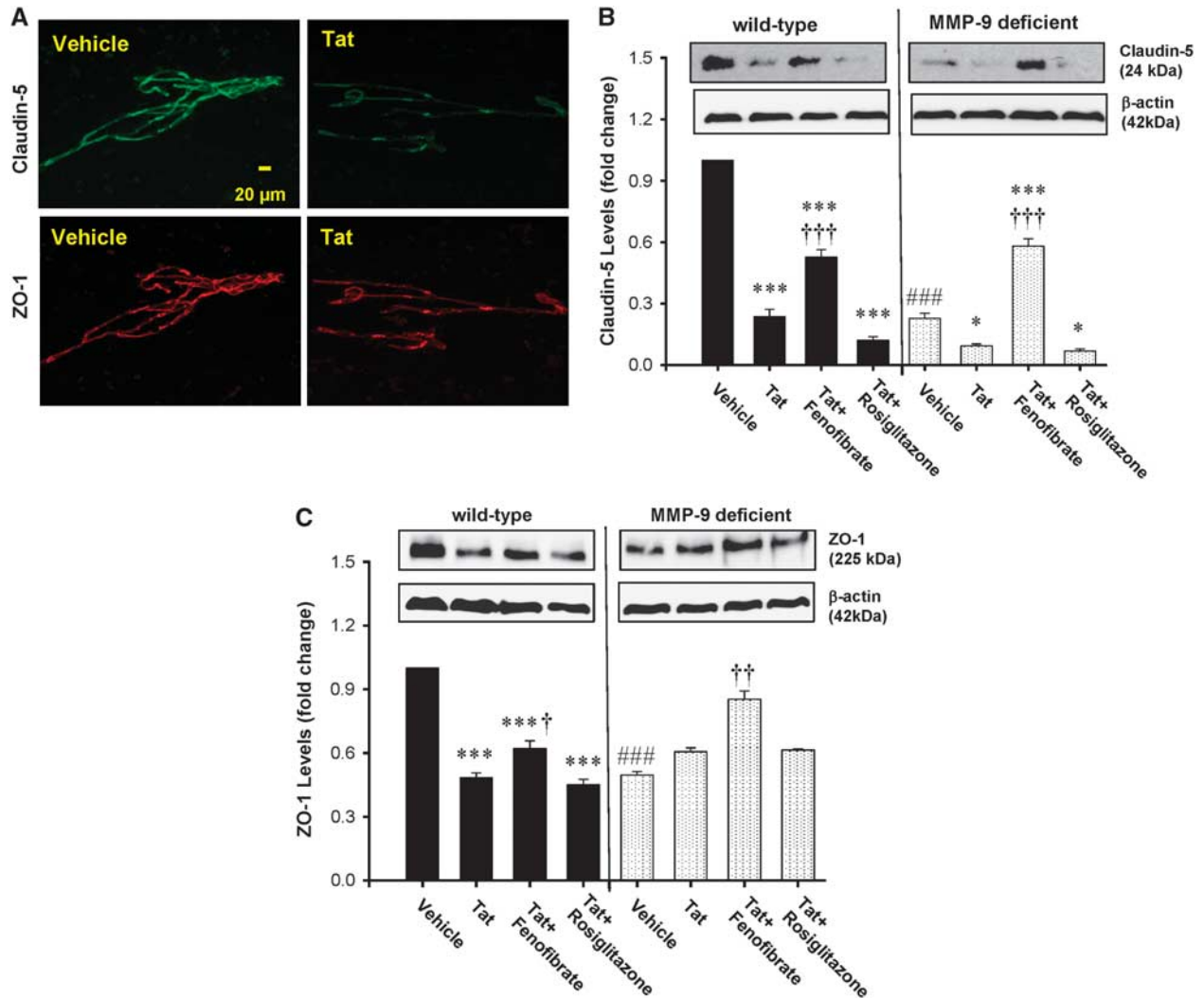


Figure 2. Tat-induced alterations in tight junction (TJ) protein expression are attenuated by peroxisome proliferator-activated receptor α (PPAR α) agonists. Wild-type (WT, FVB/NJ) mice and matrix metalloproteinase-9 (MMP-9)-deficient mice were administered with PPAR agonists, followed by exposure to HIV-1 Tat as in Figure 1 and determination of TJ proteins in brain microvessels. **(A)** Examples of Tat-induced effects on expression of claudin-5 (upper panel) and zonula occludens-1 (ZO-1) (lower panel) in isolated brain microvessels of WT mice as determined by immunofluorescence. **(B, C)** Quantification of Tat and PPAR agonist-mediated effects on claudin-5 and ZO-1 levels as determined by immunoblotting. Results are the mean \pm SEM. *Significantly different as compared with vehicle-treated controls in WT or matrix metalloproteinase-9 (MMP-9)-deficient mice at $P < 0.05$ or *** $P < 0.001$. †Results in the groups exposed to Tat plus PPAR agonist are significantly different as compared with the corresponding group exposed only to Tat at $P < 0.05$, †† $P < 0.01$, or ††† $P < 0.001$. ###Baseline (vehicle-treated) levels in MMP-9-deficient mice are statistically different as compared with control levels in WT mice at $P < 0.001$.

Determination of Astrogliosis and Neuronal Loss

Expression of NeuN in the brains was analyzed by immunoblotting and immunofluorescence as a marker of neuronal loss. For immunoblotting, the brains were homogenized in ice-cold RIPA lysis buffer (Santa Cruz Biotechnology) and centrifuged at 15,000 g for 15 minutes. The aliquots of supernatants (20 μ g of protein) were loaded onto 4% to 15% Tris-HCl Ready SDS-polyacrylamide gel (Bio-Rad Laboratories). Mouse anti-NeuN antibody was purchased from Millipore (Kankakee, IL, USA); rabbit anti-GFAP antibody and anti-actin antibody were from Sigma; and all secondary antibodies were from Santa Cruz Biotechnology.

For immunostaining analyses, the brains were removed and serial coronal sections (10 μ m each) in optimal cutting temperature compound were prepared. The staining was performed as previously described.²² The brain sections were blocked with 3% BSA in PBS and incubated with mouse anti-NeuN (1:500; Millipore) or rabbit anti-GFAP antibodies (1:500; Sigma) at 4°C overnight. After removal of primary antibodies, the sections were washed with PBS and incubated with Alexafluor 568-conjugated anti-mouse IgG or Alexafluor 488-conjugated anti-rabbit IgG (Invitrogen)

(1:1,000 dilution in 1% BSA in PBS) for 1 hour at 37°C. After final washing with PBS, slides were mounted with ProLong Gold Antifade reagent containing 4',6-diamidino-2-phenylindole (Invitrogen) to visualize the nuclei. The immunofluorescent images were evaluated and captured using confocal microscopy.

Image Quantification and Statistical Analysis

Quantification of image data was performed using the image analysis programs ImageJ (version 1.41, NIH, Baltimore, MD, USA). To minimize the variation in fluorescence intensities from image to image, we compared the absolute numbers of pixels in images, which were prepared in the same experiment with the same pool of antibodies and were taken under the identical instrument setting. Routine statistical analysis was completed using Sigma-Stat 2.03 (SPSS, Chicago, IL, USA). One- or two-way ANOVA was used to compare mean responses among the treatments. Statistical probability of $P < 0.05$ was considered as significant. All experiments and analyses were repeated at least three times.

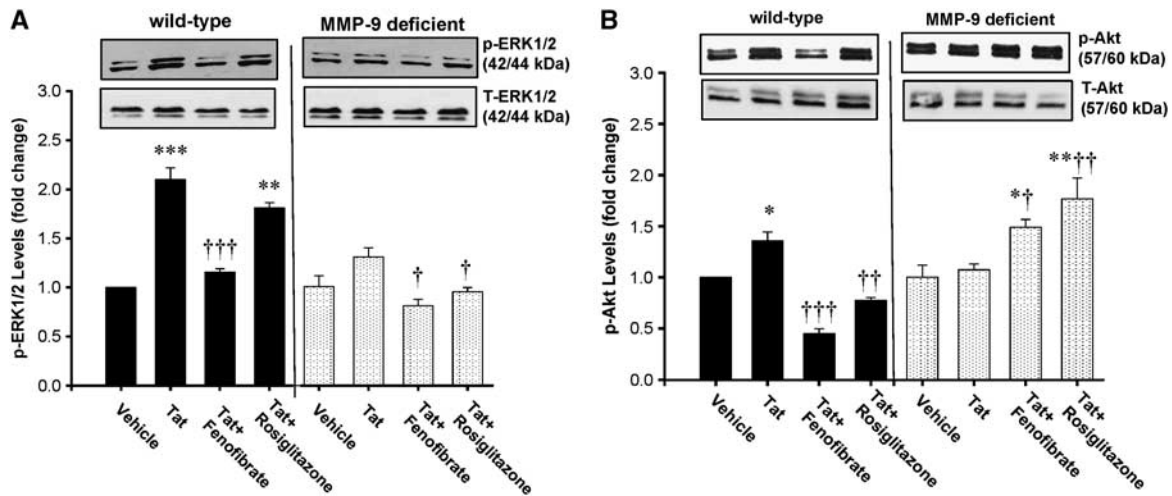


Figure 3. Peroxisome proliferator-activated receptor γ (PPAR γ) protects against HIV Tat-induced activation of the ERK1/2 and Akt signaling. Wild-type (WT, FVB/NJ) and matrix metalloproteinase-9 (MMP-9)-deficient mice were administered with PPAR agonists, followed by exposure to Tat for 24 hours as in Figure 1. Total ERK1/2 (T-ERK1/2) and phosphorylated ERK1/2 (p-ERK1/2) (A) and Akt (B) in brain microvessels were detected by immunoblotting. Molecular weight of ERK1/2 and Akt bands is indicated on the graph. The two bands in the p-ERK and T-ERK panels represent ERK1 (44 kDa) and ERK2 (42 kDa), respectively. The two bands in p-Akt and T-Akt panels represent Akt1 (60 kDa) and Akt2 (57 kDa), respectively. Results are the mean \pm SEM. *Significantly different as compared with vehicle-treated controls in WT or MMP-9-deficient mice at $P < 0.05$, ** $P < 0.01$, or *** $P < 0.001$. †Results in the groups exposed to Tat plus PPAR agonist are significantly different as compared with the corresponding group exposed only to Tat at $P < 0.05$, †† $P < 0.01$, or ††† $P < 0.001$.

RESULTS

Peroxisome Proliferator-Activated Receptor Agonists Protect Against HIV-1 Tat-Induced Disruption of Paracellular Blood–Brain Barrier Integrity

Exposure to HIV-1 Tat disrupts the BBB integrity,²³ however, the protective strategies against this effect are poorly developed. Our initial series of experiments focused on the effects of PPAR activity modulators on Tat-induced alterations of the BBB permeability in WT mice. The analyses were performed using sodium fluorescein flux from the vasculature into the brain parenchyma. In cases of severely compromised BBB integrity, increased levels of sodium fluorescein in brain tissue result in yellowing the brains (Figure 1, upper panel). As quantified in Figure 1, exposure to Tat markedly increased BBB permeability. Importantly, pretreatment with PPAR α agonist, fenofibrate, or PPAR γ agonist, rosiglitazone, attenuated Tat-induced BBB hyperpermeability. In contrast, Tat-induced disruption of the BBB integrity was further exacerbated by PPAR γ antagonist, GW9662. Cotreatment with PPAR α antagonist, MK886, did not affect Tat-mediated changes in BBB permeability.

Peroxisome Proliferator-Activated Receptor Agonists Differentially Attenuate Tat-Induced Alterations in Tight Junction Protein Expression

Tight junctions, which regulate paracellular BBB permeability, are susceptible to Tat-induced disruption via MMP-mediated mechanisms.^{14,24} Therefore, we evaluated the influence of PPAR agonists on Tat-induced changes in TJ expression levels in both WT and MMP-9-deficient mice. To focus our studies on cerebrovascular toxicity of Tat, the analyses were performed on isolated brain microvessels. We evaluated the expression levels of claudin-5, a transmembrane TJ protein, and TJ-associated protein, ZO-1, which links the transmembrane TJ proteins to the actin cytoskeleton.

Exposure to Tat for 24 hours downregulated claudin-5 and ZO-1 levels in the brain microvessels of WT. The examples of these effects are illustrated in Figure 2A. While the basal levels of TJ proteins were lower in MMP-9 $^{-/-}$ mice as compared with WT controls, treatment with Tat decreased claudin-5 but not ZO-1

levels in MMP-9-deficient mice (Figures 2B and 2C). Preexposure to PPAR agonists had differential effects on TJ protein expression as only fenofibrate, but not rosiglitazone, attenuated Tat-induced alterations in claudin-5 (Figure 2B) and ZO-1 (Figure 2C) expression in WT mice. Moreover, treatment with fenofibrate plus Tat increased TJ expression above control levels in MMP-9 $^{-/-}$ mice (Figures 2B and 2C).

Peroxisome Proliferator-Activated Receptor γ Protects Against Tat-Induced Activation of the ERK1/2 and Akt Signaling

The ERK1/2 and Akt signaling was linked to the regulation of TJ protein integrity;¹⁵ therefore, we also evaluate these pathways in the present study. Exposure to Tat markedly induced phosphorylation of ERK1/2 (Figure 3A) and Akt (Figure 3B) in brain microvessels of WT mice. In contrast, Tat induced only minimal effects on ERK1/2 phosphorylation and had no influence on Akt phosphorylation in MMP-9-deficient mice. Consistent with the data on TJ expression, exposure to fenofibrate, but not rosiglitazone, attenuated Tat-induced activation of ERK1/2 and Akt in WT mice. In MMP-9-deficient mice, both fenofibrate and rosiglitazone protected against Tat-induced phosphorylation of ERK1/2; however, fenofibrate enhanced Akt phosphorylation in these animals.

Peroxisome Proliferator-Activated Receptor Agonists Protect Against HIV-1 Tat-Induced Reactive Astroglia

One of the hallmarks of HIV-1 CNS infection is reactive astroglia, associated with increased GFAP expression. In addition, Tat was shown to activate GFAP in astrocytes.^{25,26} To evaluate whether PPAR agonists protect against Tat-induced astroglia, WT and MMP-9-deficient mice were pretreated with fenofibrate or rosiglitazone, followed by repeated Tat injections (20 μ g/mouse, 48 hours apart) into the ICA. Initial exposure to a single dose of Tat for 24 hours did not induce GFAP overexpression (data not shown). However, the repeated administration of Tat stimulated GFAP expression at day 7, as determined by immunostaining (Figure 4A) and immunoblotting (Figure 4B). While reactive astroglia in response to Tat was observed both in WT and in

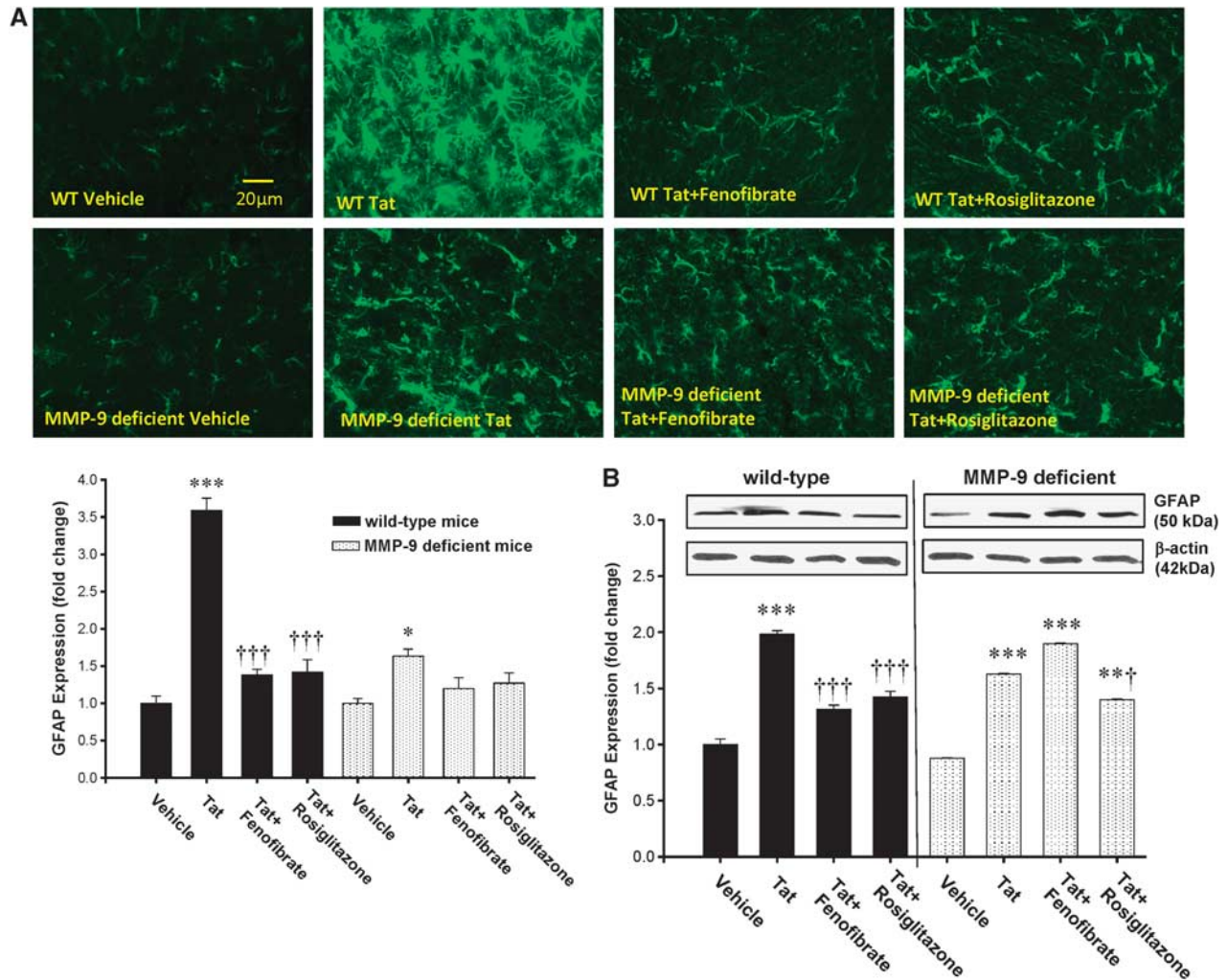


Figure 4. Peroxisome proliferator-activated receptor (PPAR) agonists protect against HIV Tat-induced reactive astrogliosis. Mice were treated with PPAR agonists as in Figure 1, followed by repeated injections with Tat (20 μ g/injection, administered every other day for the total of three injections) and determination of GFAP expression as the marker of astrogliosis by immunostaining (A) or immunoblotting (B). Images reflect representative data from at least three experiments. Analyses were performed 7 days after the first injection of Tat in the cerebral cortex (A) or the whole brain homogenates (B). Results are the mean \pm SEM. *Significantly different as compared with vehicle-treated controls in wild-type (WT) or MMP-9 $-/-$ mice at $P < 0.01$, ** $P < 0.01$, or *** $P < 0.001$. †Results in the groups exposed to Tat plus PPAR agonist are significantly different as compared with the corresponding group exposed only to Tat at $P < 0.05$ or ††† $P < 0.001$. MMP-9, matrix metalloproteinase 9.

MMP-9-deficient mice, the overall effects were markedly less pronounced in mice with MMP-9 deficiency (Figure 4A). Tat-induced GFAP overexpression was inhibited by fenofibrate and rosiglitazone in WT mice (Figures 4A and 4B). In contrast, only rosiglitazone, but not fenofibrate, attenuated Tat-induced astrogliosis in MMP-9 $-/-$ mice (Figure 4B).

Peroxisome Proliferator-Activated Receptor Agonists Protect Against HIV Tat-Induced Neuronal Loss

Neuronal injury underlies the development of cognitive dysfunction frequently observed in HIV-1 brain infection.²⁷ Therefore, we evaluated the effects of Tat and PPAR agonists on neuronal loss using NeuN as a specific neuronal marker. Exposure to Tat induced an evident neuronal loss in the cerebral cortex of WT mice 24 hours after Tat administration as determined by both immunostaining (Figure 5A) and immunoblotting (Figure 5B). Importantly, these effects were alleviated by pretreatment of mice with fenofibrate or rosiglitazone (Figures 5A and 5B). In contrast to WT mice, Tat did not induce a visible neuronal loss in MMP-9

animals. In addition, fenofibrate increased NeuN immunostaining in these mice above control levels (Figures 5A and 5B).

DISCUSSION

Increased tissue oxidative stress and upregulation of MMPs induced by Tat contribute to HIV-1-induced BBB disruption and the development of AIDS-associated dementia at later stages of HIV infection.^{14–16} Oxidative stress may also be an early step in the mechanism of Tat neurotoxicity.¹⁶ Peroxisome proliferator-activated receptor are ligand-activated transcription factors that can downregulate activation of redox-responsive transcription factors¹⁵ and exert antiinflammatory effects.⁶ Therefore, therapeutic intervention with PPAR agonists appears to be an attractive option in HIV. Indeed, the results of the present study indicated that both PPAR α and PPAR γ agonists protected against Tat-induced downregulation of TJ proteins; although fenofibrate (PPAR α agonist) was more effective in preventing activation of ERK1/1 and Akt in WT mice. These differential effects of PPAR agonists may reflect their role in metabolism and antioxidative

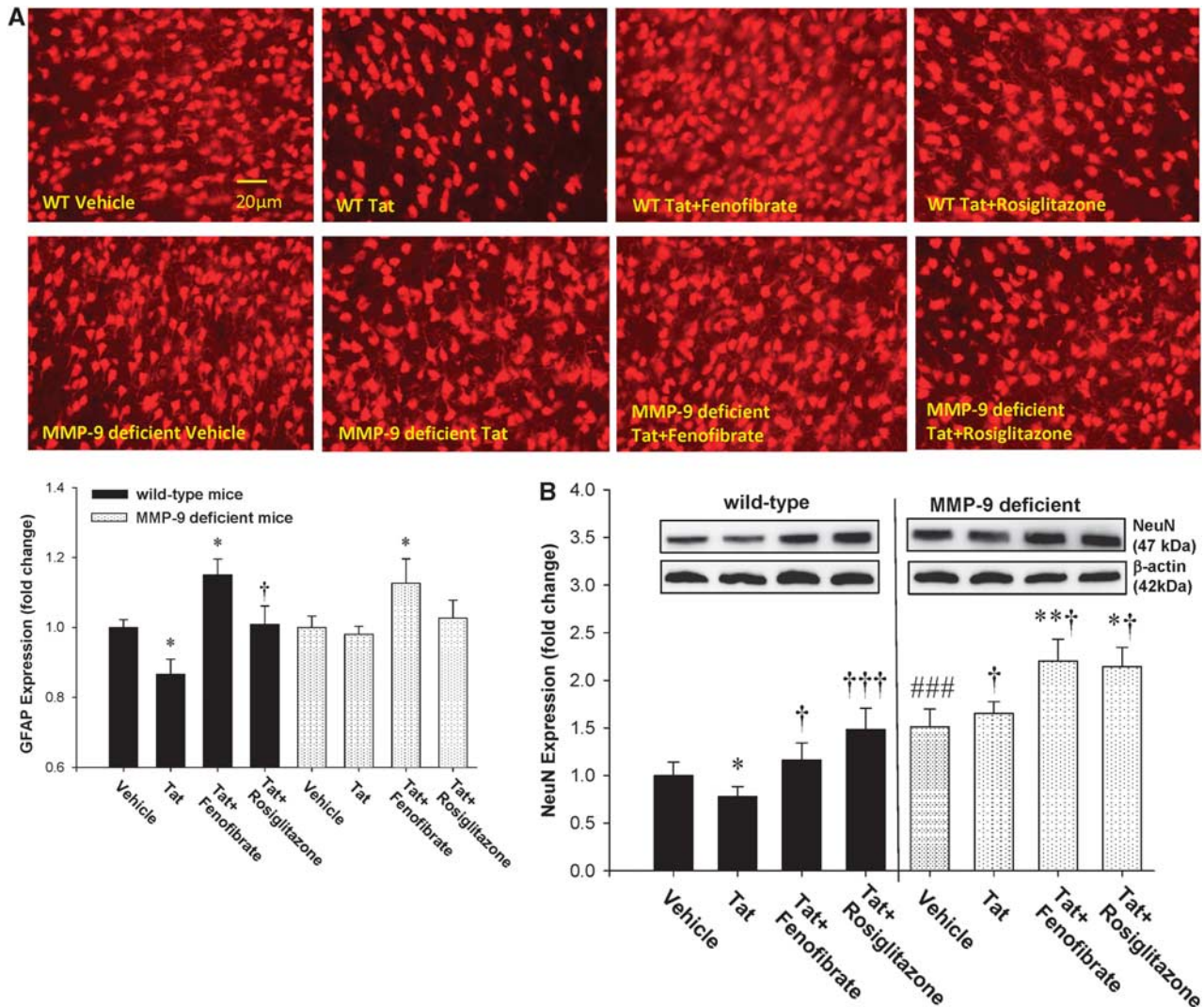


Figure 5. Peroxisome proliferator-activated receptor (PPAR) agonists protect against HIV Tat-induced neuronal loss. The expression of NeuN was decreased in the cerebral cortex of the wild-type (WT) mice at the 24-hour time point after the single dose of HIV-1 Tat. These effects were attenuated by cotreatment with fenofibrate or rosiglitazone or in the matrix metalloproteinase-9 (MMP-9) knockout mice as detected by immunofluorescent staining (A) and western blotting (B). Images reflect representative data from at least three experiments. Results are the mean \pm SEM. *Significantly different as compared with vehicle-treated controls in WT or MMP-9 $-/-$ mice at $P < 0.05$ or $**P < 0.01$. †Results in the groups exposed to Tat plus PPAR agonist are significantly different as compared with the corresponding group exposed only to Tat at † $P < 0.05$ or †† $P < 0.001$. ###Baseline (vehicle-treated) levels in MMP-9-deficient mice are statistically different as compared with control levels in WT mice at $P < 0.001$.

protection. While PPAR α is highly expressed in liver, skeletal muscle, kidney, heart, and the vascular wall, PPAR γ is predominantly detected in adipose tissue, intestine, and macrophages. Peroxisome proliferator-activated receptor α and PPAR γ have different functions on regulating lipid metabolism, cell proliferation, and differentiation. Peroxisome proliferator-activated receptor α controls intracellular and extracellular lipid metabolisms, whereas PPAR γ triggers adipocyte differentiation and promotes lipid storage.²⁸

ERK1/2 and Akt signaling as well as oxidative stress-responsive transcription factors are known to induce MMP expression.¹⁵ Our *in vitro* data showed that HIV-1-induced activation of MMP-9 was attenuated by blocking ERK and Akt signaling and that these effects were caveolae dependent.¹⁵ Among a variety of cellular functions, MMPs (and in particular MMP-9) are involved in regulation of the BBB permeability and TJ integrity.¹⁴ Therefore, part of the current studies was completed in MMP-9-deficient animals. We choose a genetic model of MMP-9 deficiency instead

of MMP inhibitors because the nonselective nature of MMP inhibitors causes several side effects that hinder their therapeutic use.²⁹ The rationale for targeting MMP-9 was also made based on the observation that this MMP involved in the development of neuroinflammation. Indeed, increased MMP secretion was shown to be involved in HIV-1 exiting the blood stream and gaining access to body tissues, and serum MMP levels correlated with brain injury in patients with advanced HIV infection.³⁰ In addition, the neurotoxicity induced by Tat was inhibited by anti-MMP antibodies, but not by antibodies against Tat, indicating that Tat causes neuronal death through an indirect mechanism.¹⁷ Our previous study indicated that Tat exposure upregulated MMP-9 protein levels in brain endothelial cells^{14,15} and administration of Tat into the ICA enhanced MMP-9 activity in plasma and protein expression in brain tissue.¹⁹ The mechanisms by which MMPs disrupt the barrier integrity of the brain endothelium appear to involve degradation of specific TJ proteins; therefore, it was surprising to show in the present study that the baseline

expression of importantly TJ proteins, such as claudin-5 and ZO-1, was lower in MMP-9 knockout mice as compared with WT controls. Nevertheless, TJ proteins in MMP-9-deficient mice were inducible as shown by treatment with fenofibrate.

While microglia are the main CNS cell type productively infected by HIV,³¹ recent evidence reevaluated the importance of astrocytes as the cells susceptible to HIV infection.³² Using *in situ* PCR, it was considered that only 1% to 3% astrocytes are infected in HIV-infected brains.^{33,34} These findings were recently revised when up to 20% infected astrocytes were detected in brains of patients with HIV-associated dementia by combining double immunohistochemistry, laser capture microdissection, and highly sensitive multiplexed PCR.³² The magnitude of astrocyte infection was also correlated with the severity of HIV-associated dementia and HIV-associated encephalitis. In addition, extensive reactive astrogliosis, neuronal loss, and formation of multinucleated giant cells from fusion of infected microglia are characteristic for the brain infection by HIV in AIDS patients.^{35,36} Several of these findings can be reproduced by exposing experimental animals to Tat protein. For example, reactive astrogliosis, which is considered as a pathologic hallmark of brain injury,³⁷ was found in the striatum as late as 7 days after a single microinjection of 50 µg Tat 1 to 72 into striatum via stereotaxic injection.¹⁶ In the current study, Tat also induced a late effect on overexpression of GFAP, which was attenuated by PPAR agonists and MMP-9 deficiency.

An intact synaptodendritic network is vital for normal cognitive functioning. Even though HIV does not replicate in neurons, neuronal death and synaptodendritic degenerative changes highlight neurocognitive dysfunctions, which frequently develop during the CNS infection by HIV.³⁸ This phenomenon also illustrates the fact that neuronal dysfunction and death are not caused directly by HIV but rather result from indirect factors, such as release of viral proteins, inflammatory mediators, and other factors from infected cells. In the present study, injection of Tat into cerebral vasculature induced a prominent neuronal loss in WT mice. However, PPAR agonists and MMP-9 deficiency attenuated these effects, mirroring their influence on Tat-induced astrogliosis. Molecular mechanisms of interactions of PPAR agonists with MMP-9 are not fully understood. We showed that transcriptional regulation of MMP-9 expression requires functional caveolae and is modulated by PPAR α or PPAR γ via ERK and Akt signaling.^{14,15} In addition, a recent study provided evidence that MMP-9 can be directly regulated by yet another PPAR isoform, PPAR δ . It was also showed that PPAR response element is present in the promoter region of MMP-9 at the location -944 to -921 bp and its binding to PPAR δ is responsible for transrepression of MMP-9 expression.³⁹

In conclusion, the results of the present study indicate the therapeutic properties of PPAR agonists in HIV-induced brain pathology with the focus on their protective effects against cerebrovascular toxicity. Interestingly, stimulation of PPAR α activity appears to be more protective as compared with PPAR γ . Matrix metalloproteinase-9 deficiency further potentiated protective effects of PPAR α agonists fenofibrate, indicating the importance of multitarget approach for a better protection against Tat-induced cerebrovascular damage.

DISCLOSURE/CONFLICT OF INTEREST

The authors declare no conflict of interest.

REFERENCES

- Alfahad TB, Nath A. Update on HIV-associated neurocognitive disorders. *Curr Neurol Neurosci Rep* 2013; **13**: 387.
- Valcour V, Paul R. HIV infection and dementia in older adults. *Clin Infect Dis* 2006; **42**: 1449–1454.
- Clotet B, Negredo E. HIV protease inhibitors and dyslipidemia. *AIDS Rev* 2003; **5**: 19–24.
- Cedeno-Laurent F, Penalva de Oliveira AC, Vidal JE, Trujillo JR. Human polyomavirus-associated cerebral disorders in the post-HAART era. *Patholog Res Int* 2011; **2011**: 562427.
- Jiang B, Hebert VY, Li Y, Mathis JM, Alexander JS, Dugas TR. HIV antiretroviral drug combination induces endothelial mitochondrial dysfunction and reactive oxygen species production, but not apoptosis. *Toxicol Appl Pharmacol* 2007; **224**: 60–71.
- Huang W, Rha GB, Han MJ, Eum SY, Andras IE, Zhong Y et al. PPAR α and PPAR γ effectively protect against HIV-induced inflammatory responses in brain endothelial cells. *J Neurochem* 2008; **107**: 497–509.
- van Wijk JP, de Koning EJ, Cabezas MC, op't Roodt J, Joven J, Rabelink TJ et al. Comparison of rosiglitazone and metformin for treating HIV lipodystrophy: a randomized trial. *Ann Intern Med* 2005; **143**: 337–346.
- Ramirez SH, Heilman D, Morsey B, Potula R, Haorah J, Persidsky Y. Activation of peroxisome proliferator-activated receptor gamma (PPAR γ) suppresses Rho GTPases in human brain microvascular endothelial cells and inhibits adhesion and transendothelial migration of HIV-1 infected monocytes. *J Immunol* 2008; **180**: 1854–1865.
- Potula R, Ramirez SH, Knipe B, Leibhart J, Schall K, Heilman D et al. Peroxisome proliferator-activated receptor-gamma activation suppresses HIV-1 replication in an animal model of encephalitis. *AIDS* 2008; **22**: 1539–1549.
- McCoig C, Castrejon MM, Saavedra-Lozano J, Castano E, Baez C, Lanier ER et al. Cerebrospinal fluid and plasma concentrations of proinflammatory mediators in human immunodeficiency virus-infected children. *Pediatr Infect Dis J* 2004; **23**: 114–118.
- Sporer B, Paul R, Koedel U, Grimm R, Wick M, Goebel FD et al. Presence of matrix metalloproteinase-9 activity in the cerebrospinal fluid of human immunodeficiency virus-infected patients. *J Infect Dis* 1998; **178**: 854–857.
- Mastroianni CM, Liuzzi GM. Matrix metalloproteinase dysregulation in HIV infection: implications for therapeutic strategies. *Trends Mol Med* 2007; **13**: 449–459.
- Hsieh HL, Wang HH, Wu WB, Chu PJ, Yang CM. Transforming growth factor-beta1 induces matrix metalloproteinase-9 and cell migration in astrocytes: roles of ROS-dependent ERK- and JNK-NF-kappaB pathways. *J Neuroinflammation* 2010; **7**: 88.
- Huang W, Eum SY, Andras IE, Hennig B, Toborek M. PPAR α and PPAR γ attenuate HIV-induced dysregulation of tight junction proteins by modulations of matrix metalloproteinase and proteasome activities. *FASEB J* 2009; **23**: 1596–1606.
- Huang W, Andras IE, Rha GB, Hennig B, Toborek M. PPAR α and PPAR γ protect against HIV-1-induced MMP-9 overexpression via caveolae-associated ERK and Akt signaling. *FASEB J* 2011; **25**: 3979–3988.
- Aksenov MY, Hasselrot U, Wu G, Nath A, Anderson C, Mactutus CF et al. Temporal relationships between HIV-1 Tat-induced neuronal degeneration, OX-42 immunoreactivity, reactive astrogliosis, and protein oxidation in the rat striatum. *Brain Res* 2003; **987**: 1–9.
- Chao C, Ghorpade A. Production and roles of glial tissue inhibitor of metalloproteinases-1 in human immunodeficiency virus-1-associated dementia neuroinflammation: a review. *Am J Infect Dis* 2009; **5**: 314–320.
- Huang W, Rha GB, Chen L, Seelbach MJ, Zhang B, András IE et al. Inhibition of telomerase activity alters tight junction protein expression and induces transendothelial migration of HIV-1-infected cells. *Am J Physiol Heart Circ Physiol* 2010; **298**: H1136–H1145.
- Chen L, Choi JJ, Choi YJ, Hennig B, Toborek M. HIV-1 Tat-induced cerebrovascular toxicity is enhanced in mice with amyloid deposits. *Neurobiol Aging* 2012; **33**: 1579–1590.
- Johnson TP, Patel K, Johnson KR, Maric D, Calabresi PA, Hasbun R et al. Induction of IL-17 and nonclassical T-cell activation by HIV-Tat protein. *Proc Natl Acad Sci USA* 2013; **110**: 13588–13593.
- Chen L, Swartz KR, Toborek M. Vessel microport technique for applications in cerebrovascular research. *J Neurosci Res* 2009; **87**: 1718–1727.
- Seelbach MJ, Brooks TA, Egleton RD, Davis TP. Peripheral inflammatory hyperalgesia modulates morphine delivery to the brain: a role for P-glycoprotein. *J Neurochem* 2007; **102**: 1677–1690.
- Pu H, Tian J, Andras IE, Hayashi K, Flora G, Hennig B et al. HIV-1 Tat protein-induced alterations of ZO-1 expression are mediated by redox-regulated ERK 1/2 activation. *J Cereb Blood Flow Metab* 2005; **25**: 1325–1335.
- Xu R, Feng X, Xie X, Zhang J, Wu D, Xu L. HIV-1 Tat protein increases the permeability of brain endothelial cells by both inhibiting occludin expression and cleaving occludin via matrix metalloproteinase-9. *Brain Res* 2012; **1436**: 13–19.
- Zou W, Wang Z, Liu Y, Fan Y, Zhou BY, Yang XF. Involvement of p300 in constitutive and HIV-1 Tat-activated expression of glial fibrillary acidic protein in astrocytes. *Glia* 2010; **58**: 1640–1648.
- Zhou BY, Liu Y, Kim B, Xiao Y, He JJ. Astrocyte activation and dysfunction and neuron death by HIV-1 Tat expression in astrocytes. *Mol Cell Neurosci* 2004; **27**: 296–305.

- 27 Harezlak J, Buchthal S, Taylor M, Schifitto G, Zhong J, Daar E *et al*. Persistence of HIV-associated cognitive impairment, inflammation, and neuronal injury in era of highly active antiretroviral treatment. *AIDS* 2011; **25**: 625–633.
- 28 Hummasti S, Tontonoz P. The peroxisome proliferator-activated receptor N-terminal domain controls isotype-selective gene expression and adipogenesis. *Mol Endocrinol* 2006; **20**: 1261–1275.
- 29 Roycik MD, Myers JS, Newcomer RG, Sang QX. Matrix metalloproteinase inhibition in atherosclerosis and stroke. *Curr Mol Med* 2013; **13**: 1299–1313.
- 30 Ragin AB, Wu Y, Ochs R, Scheidegger R, Cohen BA, McArthur JC *et al*. Serum matrix metalloproteinase levels correlate with brain injury in human immunodeficiency virus infection. *J Neurovirol* 2009; **15**: 275–281.
- 31 Bertin J, Barat C, Belanger D, Tremblay MJ. Leukotrienes inhibit early stages of HIV-1 infection in monocyte-derived microglia-like cells. *J Neuroinflammation* 2012; **9**: 55.
- 32 Churchill MJ, Wesselingh SL, Cowley D, Pardo CA, McArthur JC, Brew BJ *et al*. Extensive astrocyte infection is prominent in human immunodeficiency virus-associated dementia. *Ann Neurol* 2009; **66**: 253–258.
- 33 Bagasra O, Lavi E, Bobroski L, Khalili K, Pestaner JP *et al*. Cellular reservoirs of HIV-1 in the central nervous system of infected individuals: identification by the combination of in situ polymerase chain reaction and immunohistochemistry. *AIDS* 1996; **10**: 573–585.
- 34 Takahashi K, Wesselingh SL, Griffin DE, McArthur JC, Johnson RT, Glass JD. Localization of HIV-1 in human brain using polymerase chain reaction/in situ hybridization and immunocytochemistry. *Ann Neurol* 1996; **39**: 705–711.
- 35 Kramer-Hammerle S, Rothenaigner I, Wolff H, Bell JE, Brack-Werner R. Cells of the central nervous system as targets and reservoirs of the human immunodeficiency virus. *Virus Res* 2005; **111**: 194–213.
- 36 Bell JE. An update on the neuropathology of HIV in the HAART era. *Histopathology* 2004; **45**: 549–559.
- 37 Maragakis NJ, Rothstein JD. Mechanisms of Disease: astrocytes in neurodegenerative disease. *Nat Clin Pract Neurol* 2006; **2**: 679–689.
- 38 Sacktor N, Lyles RH, Skolasky R, Kleeberger C, Selnes OA, Miller EN *et al*. HIV-associated neurologic disease incidence changes: Multicenter AIDS Cohort Study, 1990–1998. *Neurology* 2001; **56**: 257–260.
- 39 Yin KJ, Deng Z, Hamblin M, Zhang J, Chen YE. Vascular PPAR δ protects against stroke-induced brain injury. *Arterioscler Thromb Vasc Biol* 2011; **31**: 574–581.